Magnetic and transport properties of epitaxial films of $SrRuO_3$ in the ultrathin limit

Moty Schultz,[1] Shahar Levy,[1] James W. Reiner,[2] and Lior Klein[1]
[1]*Department of Physics, Nano-magnetism Research Center, Institute of Nanotechnology and Advanced Materials, Bar-Ilan University, Ramat-Gan 52900, Israel*
[2]*Department of Applied Physics, Yale University, New Haven, Connecticut 06520-8284, USA*
(Received 14 December 2008; revised manuscript received 15 February 2009; published 31 March 2009)

We measured ultrathin epitaxial films of the itinerant ferromagnet $SrRuO_3$ to study effects of decreasing film thickness on transport and magnetic properties. We find that the resistivity ratio decreases, the ferromagnetic phase transition occurs at a lower Curie temperature, and the easy axis of magnetization rotates toward a more perpendicular orientation. We discuss possible interpretations of the observed behavior.

DOI: 10.1103/PhysRevB.79.125444 PACS number(s): 73.50.−h, 72.15.Gd, 75.40.Cx

I. INTRODUCTION

Finite-size effects in films of itinerant ferromagnets are intrinsically complex since in addition to effects exhibited by nonmagnetic metals, (e.g., increased effects of electron-electron correlation) there are effects particular to magnetic metals that occur, for instance, when the magnetic correlation length becomes comparable to one of the dimensions of the sample. For these reasons, finite-size effects in magnetic films have attracted for several decades considerable interest which has intensified in recent years in view of the use of nanometer-thick films and submicron patterns in novel spintronic devices.

Much of the study in this field has concentrated on 3*d* ferromagnetic alloys which are good metals and soft ferromagnets. Here, we explore the effect of film thickness in $SrRuO_3$—a 4*d* itinerant ferromagnet known for its "bad" metal properties[1–4] and extremely large uniaxial magnetocrystalline anisotropy (MCA).[5] Exploring this compound not only provides the opportunity of studying finite-size effects in a qualitatively different system; due to the fact that epitaxial thin films of $SrRuO_3$ grow epitaxially on various perovskite substrates[6,7] and various perovskites can be grown on them, $SrRuO_3$ is attractive for possible multilayer device applications where the $SrRuO_3$ layer may be only few nanometer thick.

Previous studies of ultrathin $SrRuO_3$ films and $SrRuO_3/SrTiO_3$ superlattices addressed the suppression of the Curie temperature and the appearance of a metal-insulator transition.[8–11] The observations were attributed to effects of disorder,[8] strain,[10] and finite-size effects.[11] In this paper, we report on the film-thickness dependence of magnetic and transport properties of $SrRuO_3$. We find higher resistivity when the film thickness is decreased and our analysis suggests increased effects of electron-electron correlations. We also find that the ferromagnetic phase transition occurs at a lower Curie temperature (T_C) for thinner films and we attributed this behavior to finite-size effects. The extracted critical exponents are consistent with the universality class of three-dimensional (3D) Ising, while hints of dimensional crossover very close to T_C are not conclusive. The magnetic anisotropy is also affected by film thickness and the easy axis (EA), normally at 45° to the film normal, becomes parallel to the normal in 3 nm thick films.

II. EXPERIMENTAL DETAILS

Our samples are epitaxial thin films of $SrRuO_3$ grown on slightly miscut (~2°) substrates of $SrTiO_3$ by reactive electron-beam evaporation from individual Sr and Ru sources. Achieving full oxygen stoichiometry was a priority during growth, so an electron cyclotron resonance atomic oxygen source was used. The pressure at the substrate surface was 1×10^{-4} Torr. Growth rate control and calibration were achieved with a quartz microbalance and element specific atomic absorption feedback control. These growth rates were about 2 A/s and were calibrated against finite-thickness oscillations observed in x-ray diffraction (XRD) studies of 50–100 nm films.[12] These XRD studies also demonstrated that the $SrRuO_3$ films are untwined orthorhombic single crystals, with lattice parameters of $a\cong5.53$ Å, $b\cong5.57$ Å, and $c\cong7.85$ Å. The [001] direction is in the plane of the film and the [010] direction is at 45° out of the film plane.

The substrates are 5×5 mm^2 and the substrate to source distance is large for a molecular-beam epitaxy system, about 16 inches, so the expected uniformity across a 5 mm substrate is quite high (less than 0.1% variation).

We patterned the films by conventional photolithography to allow precise measurements of longitudinal and transverse resistivity. A sketch of the patterned film is shown in Fig. 1. The thickness (d) of the samples whose measurements are presented in this study is in the range of 3–27 nm. The thin samples exhibit high residual resistivity ratio (RRR) defined as $\rho(300\ \mathrm{K})/\rho(2\ \mathrm{K})$. The values of the RRR vary between 1.8 to 14.4 for thicknesses of 3 and 13.5 nm, respectively. Thicker films grown in similar conditions exhibit RRR comparable to the best single crystals available, around 90. The high values of the RRR are an important indication of the high quality of the films as they reflect a low amount of disorder (the resistivity at low temperatures has proven to be the most sensitive indicator of film stoichiometry).

III. TRANSPORT PROPERTIES

Figure 1 shows the temperature dependence of the resistivity ρ of films with thicknesses between 3 to 13.5 nm. With decreasing thickness we observe a systematic increase in resistivity and a decrease in the RRR. In addition, the kink in the resistivity (correlated with the ferromagnetic phase tran-

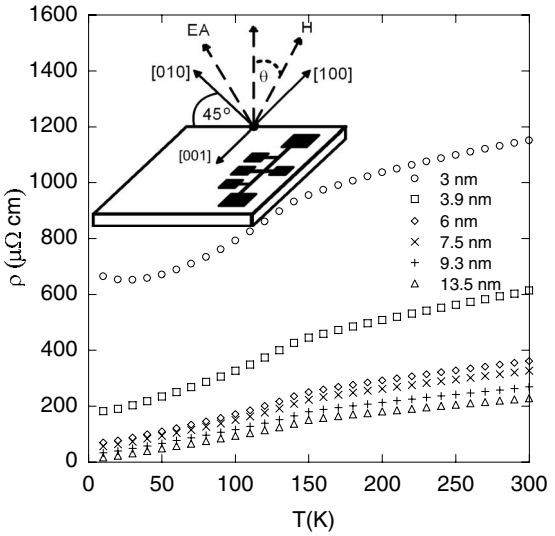

FIG. 1. Resistivity as a function of temperature for six films with different thicknesses. Inset: A sketch of the patterned film. The growth orientation of $SrRuO_3$ and the definition of the angle θ.

sition) is pushed to lower temperatures and becomes less pronounced. While previous reports show a metal-insulator transition at thicknesses 4–6 monolayers (MLs) (Refs. 8 and 9) and 4 nm,[10] our samples remain metallic down to 3 nm, presumably due to less disorder.

Various sources may be responsible to increased resistivity in the ultrathin limit including the existence of surface dead layers, increased role of surface scattering, increased strength of electron-electron interactions, band changes, etc. In the following we consider these possibilities.

Dead layer. Lattice strain and surface oxidation may induce structural defects in film layers close to the film/substrate or film/vacuum interface, making these layers insulating.[13,14] In this scenario, if d is the thickness of the film, d^* is the dead layer thickness, and σ^* is the real value of the conductivity, then *the measured conductivity* σ is given by $\sigma=\sigma^*-\frac{\sigma^* d^*}{d}$. Figure 2(a) shows the normalizes conductivity as a function of $1/d$ for four different temperatures. In our analysis we refer to measurements above 100 K where thickness dependence remains similar. We find that the data points deviate systematically from the linear fit with $d^* \sim 2$ nm [Fig. 2(b)].

Surface scattering. The relative weight of surface scattering increases when the mean-free path (l) becomes comparable to the film thickness (d). As discussed by Fuchs[15] and Sondheimer[16] the resistivity in this limit is given by

$$\rho = \rho_0 \left[1 + \frac{3}{8}(1-p)\frac{l}{d} \right] \quad (d > l), \tag{1}$$

where ρ_0 is the bulk resistivity, ρ is the measured value, and p is the specularity parameter. As demonstrated in Fig. 3, the fit is poor.

Dead layer combined with surface scattering. If both dead layer and surface scattering are taken into consideration, Eq. (1) is modified by replacing d with $d-d^*$. While the fits improve (see Fig. 4), the extracted mean-free path ($\approx$10 nm at 300 K) is inconsistent with other estimates[1] and the dead layer thickness is $\approx$2 nm.

The failure of these models suggests important role of other effects: band changes, increase in electron-electron correlations, or complicated disorder at the surface already observed with atomic force microscope (AFM).[8–10]

IV. MAGNETIC PROPERTIES

A. Magnetic anisotropy

Epitaxial thin films of $SrRuO_3$ are characterized by a single EA whose orientation is temperature dependent. Above T_C the easy axis coincides with [010] which is at 45° relative to the film normal, while below T_C there is an orientational transition where the EA rotates in the (001) plane approaching $\sim$30° relative to the normal at 2 K.[2]

To determine the magnetic anisotropy of ultrathin films, we have used both magnetization and magnetotransport measurements. The magnetization measurements were performed with a Quantum Design superconducting quantum interference device (SQUID) magnetometer capable of measuring longitudinal and transverse magnetic moments. The sample was cooled in a 1 T magnetic field in the $[\bar{1}10]$ direction down to 2 K where the field was turned off. Afterwards, the transverse and longitudinal moments were measured as a function of temperature between 2 K and T_C. The EA direction extracted from the ratio of the longitudinal and transverse moments is shown in Fig. 5(a). Due to the low signal (particularly in the thinnest films), complementary magnetotransport measurements were performed—particularly, extraordinary Hall-effect (EHE) measurements.

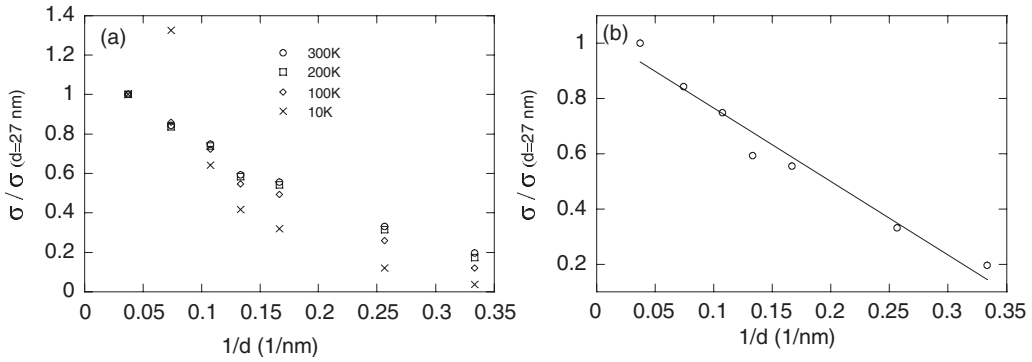

FIG. 2. (a) The normalized conductivity as a function of $1/d$ at 300, 200, 100, and 10 K. (b) Linear fit to the 300 K data.

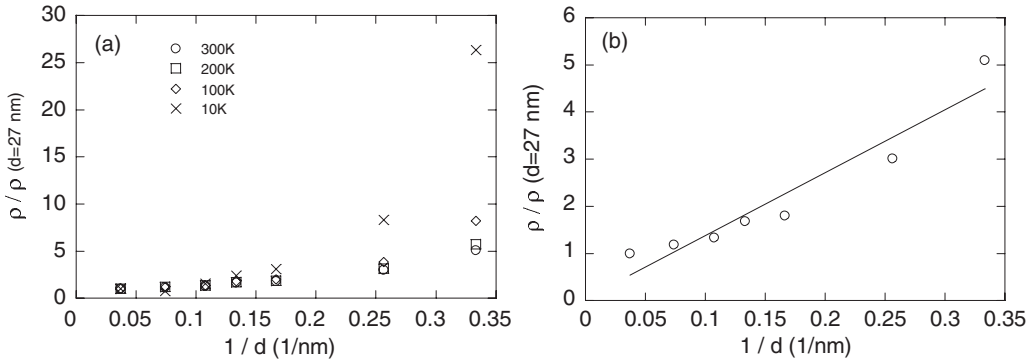

FIG. 3. (a) Variation in the normalize resistivity as a function of $1/d$ at 300, 200, 100, and 10 K. (b) Linear fit to the 300 K data.

The Hall resistivity (ρ_H) in magnetic metals has two sources: $\rho_H = R_0 B_\perp + R_s \mu_0 M_\perp$, where $B_\perp$ and $M_\perp$ are the normal (to the film plane) components of **B** and **M**, respectively, and R_0 and R_s are the ordinary and extraordinary Hall coefficients, respectively. To find the EA direction we rotate the sample in the (001) plane forward and backward relative to an applied magnetic field. As the field is rotated away from the EA, the magnetization also deviates from the EA, but it does not follow the field because of the large magnetic anisotropy. When the angle between the field and the EA exceeds 90°,[17] the magnetization abruptly reverses its orientation, which yields jumps in the Hall resistivity [see Fig. 5(b)]. Based on symmetry consideration the EA is 90° away from the average angle obtained in clockwise and anticlockwise rotations.

The results indicate that down to $d=7.5$ nm there is no change in the orientational transition, while for 5.4 nm the transition is between 40° to ~26° relative to the normal at 139 and 5 K, respectively [see Fig. 5(a)]. For the thinnest film, $d=3$ nm, the EA is perpendicular to the film plane for all temperatures below T_C.

The phenomenon that below a certain thickness the EA becomes more perpendicular is quite ubiquitous in ultrathin magnetic films, although in most cases the transition is from in-plane magnetization to perpendicular magnetization.[18–25] Models attribute the orientational transition, to competition between dipole interaction (which favors an in-plane magnetization), and surface anisotropy (which favors a perpendicular magnetization).[26–28]

We note that the critical thickness for the orientational transition of our samples (≈10 MLs) is similar to the critical thickness in other films: ≈4.9 MLs in Fe/Ag(100), ≈6.1 MLs in Fe/Cu(100),[24] ≈5.5 MLs in Co/Pd(111), and ≈12.5 MLs in Co/Pt(111).[20,21]

Qualitatively, the observed changes in the EA direction as a function of temperature and film thickness can be understood in terms of two competing sources of anisotropy: a uniaxial MCA at [010] direction (45° out of the film planes) and a uniaxial surface anisotropy normal to the film plane—both change as a function of film thickness and temperature. Since the orientational transition occurs only below T_C it is likely to be related to the spontaneous magnetization.

B. Magnetic phase transition

The advantage of using magnetotransport measurements to study the ferromagnetic phase transition in thin films of $SrRuO_3$ (Ref. 29) becomes even more evident when the films are ultrathin.

The value of T_C is readily extracted from resistivity measurements as the resistivity of itinerant ferromagnets has a kink near T_C—a manifestation of critical divergence of $\frac{d\rho}{dT}$. In $SrRuO_3$, this divergence is anomalously large, making it a useful indication of T_C.[2,3]

Figure 6 shows $\frac{d\rho}{dT}$ data of our samples and Fig. 7 shows the decreasing T_C (extracted from $\frac{d\rho}{dT}$ data) as a function of the number of MLs where a single ML is the distance between two ruthenium ions (~4 Å). Similar decrease in T_C has been observed in other ferromagnetic thin films.[30,31] Previously, this behavior in $SrRuO_3$ was attributed to extrinsic effects such as internal defects, disorder, cell compression, and thickness variations, which become more important in

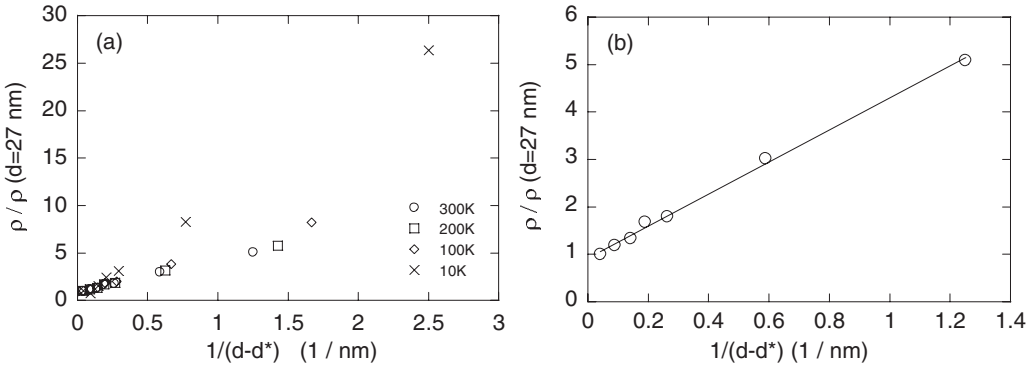

FIG. 4. (a) The same data as in Figs. 2 and 3 presented as a function of $1/(d-d^*)$. (b) Linear fit to the 300 K data.

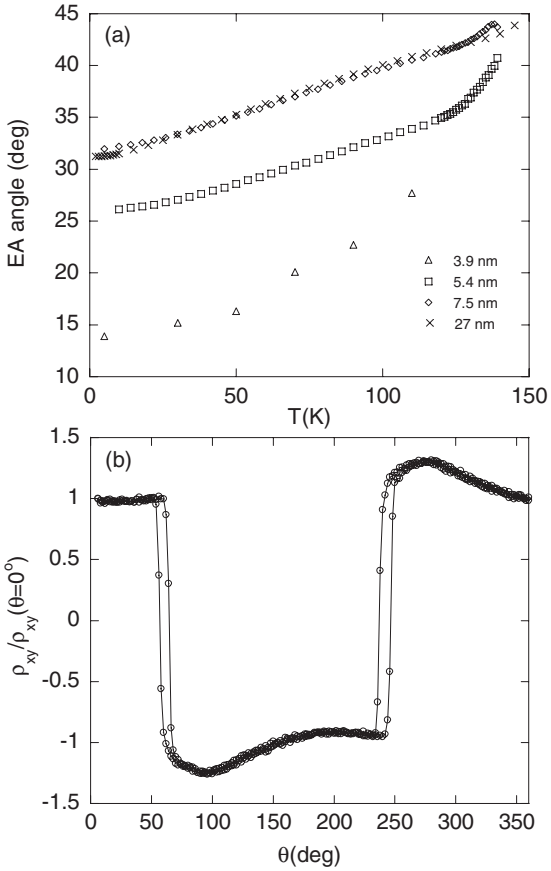

FIG. 5. (a) The easy axis direction relative to the film normal as a function of temperature of four films with different thicknesses. (b) Hall effect of a single-orientation film (3.9 nm) as a function of the magnetic field direction [θ is measured relative to the normal to the film, in the (001) plane] at $T=125$ K, $H=1$ T. (The two curves correspond to sweeps clockwise and anticlockwise in the angle.)

the ultrathin limit.[8,10] Here, we examine if intrinsic effects related to finite-size scaling are sufficient to explain these observations as already observed in $SrRuO_3/SrTiO_3$ superlattices.[11]

Near T_C, the correlation length, ξ, is given by the correlation length function

$$\xi = \xi_0 |t|^{-\nu}, \tag{2}$$

where t is the reduced temperature $(T-T_C)/T_C$ and ν is the critical exponent. According to finite-size scaling the Curie temperature when the film thickness is d $[T_C(d)]$ is the temperature at which $\xi=d$, namely, $d=\xi_0|(T_C(d)-T_C)/T_C|^{-\nu}$.[32–34] From the log-log plot of the finite-size scaling expression, as shown in the inset of Fig. 7, we find that $\nu \approx 0.86 \pm 0.03$ and the value of ξ_0, a microscopic length scale, is ≈ 1.4 Å, which is smaller than the distance between the ruthenium atoms. This emphasizes the local character of the magnetic moments in $SrRuO_3$ despite being an itinerant ferromagnet. In addition, ν is lower than the value $\nu=1$ of two-dimensional (2D) Ising universality class and higher than the value $\nu=0.64$ expected for $SrRuO_3$, which belongs to 3D Ising universality class.[29]

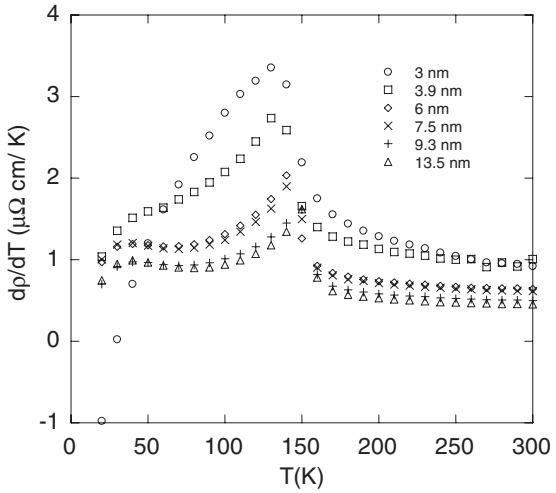

FIG. 6. $\frac{d\rho}{dT}$ as a function of temperature for six films with different thicknesses.

To further explore finite-size effects on the nature of the phase transition, we examine if the critical exponent β is affected by film thickness. For this we employ a method discussed in detail elsewhere[29] for determining the part of the resistivity related to the spontaneous magnetization $\Delta\rho_{sp}$. This method relies on the fact that above T_C the change in resistivity has nonmagnetic origin. Assuming that the behavior of the nonmagnetic resistivity is not affected by the ferromagnetic phase transition, its behavior below T_C can be approximated by an extrapolation of the resistivity above T_C. We then identify $\Delta\rho_{sp}$ as the difference between the extrapolated resistivity and the measured resistivity (see Fig. 8). This difference is related to the spontaneous magnetization.

Series expansion of $\Delta\rho_{sp}$ in powers of the spontaneous magnetization would leave for symmetry consideration only even powers, so the lowest approximation yields $\Delta\rho_{sp} \approx M_{sp}^2$. Since $M_{sp} \propto |t|^{\beta}$ we expect $\Delta\rho_{sp} \propto |t|^{2\beta}$.

Figure 9 shows $\ln \Delta\rho_{sp}$ as a function of $\ln|t|$ and we expect that the slope of the graph will be 2β.

In the inset of Fig. 9 we compare the extracted values of the critical exponent with values expected for different universality classes: 3D Ising and 2D Ising. The comparison suggests 3D Ising behavior even in the thinnest film (3 nm).

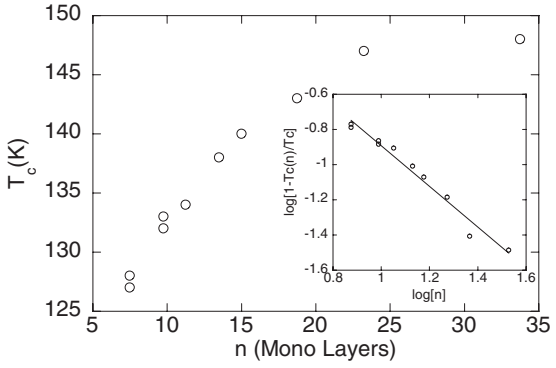

FIG. 7. The Curie temperature as a function of the number of MLs. Inset: The log-log plot of the finite-size scaling expression. The line is a fit to a linear function.

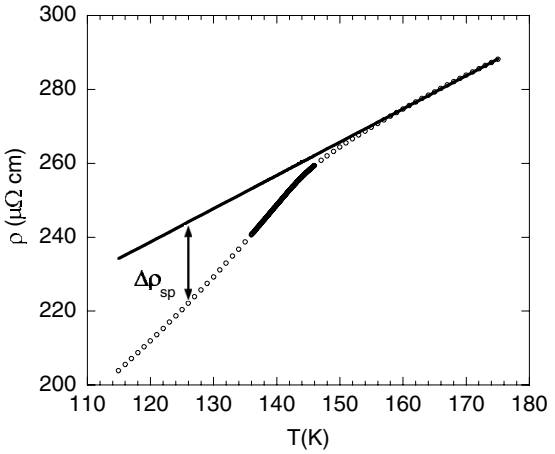

FIG. 8. Temperature dependence of the resistivity near T_C. The solid line is the extrapolation of the resistivity from $T>T_C$. The definition of $\Delta\rho_{sp}$ is shown.

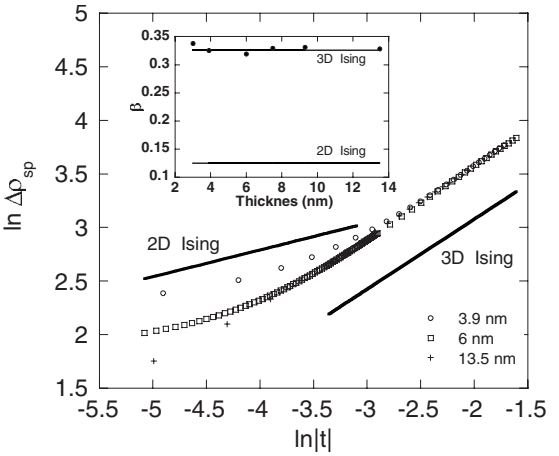

FIG. 9. Critical behavior of $\Delta\rho_{sp}$ with respect to the reduced temperature $t=(T-T_C)/T_C$ (the graphs were shifted vertically for clarity). The slope of the graph is twice the value of the critical exponent β. The solid lines have the expected slopes for 2D Ising and 3D Ising. Inset: The critical exponent β for samples with different thicknesses. The solid lines are the expected values from the theoretical methods 3D Ising and 2D Ising.

Based on the values of ξ_0 and ν we may expect a 3D-2D crossover at $|t|\approx 0.02$. Our measurements do not provide a conclusive evidence for the occurrence of this crossover. Although Fig. 9 shows a change in slope, it does not stabilize on a different slope value and it looks more like a continuous change, which may be related to extrinsic sources such as a distribution of T_C due to small and unavoidable variations in film thickness.

V. SUMMARY

We measured ultrathin epitaxial films of the itinerant ferromagnet $SrRuO_3$ to study effects of decreasing film thickness on transport and magnetic properties. Analysis of the changes in the resistivity as a function of thickness may suggest increased effects of electron-electron correlations. The decrease in the Curie temperature which occurs concomitantly with the smearing of the transition can be attributed to finite-size effects without the need to consider other effects. The extracted critical exponents ν is between the value of 3D Ising universality class and 2D Ising universality class. The critical exponent β is consistent with the universality class of 3D Ising and hints of dimensional crossover very close to T_C are not conclusive. The magnetic anisotropy is affected by film thickness and the EA, at 45° to the film normal in thick films, becomes below a certain threshold of film thickness more perpendicular. For the thinnest film, 3 nm, the EA is perpendicular to the film plane for all temperatures below T_C.

ACKNOWLEDGMENTS

L.K. acknowledges support by the Israel Science Foundation founded by the Israel Academy of Sciences and Humanities. J.W.R. grew the samples at Stanford University in the laboratory of M.R. Beasley.

[1] P. B. Allen, H. Berger, O. Chauvet, L. Forro, T. Jarlborg, A. Junod, B. Revaz, and G. Santi, Phys. Rev. B **53**, 4393 (1996).
[2] L. Klein, J. S. Dodge, C. H. Ahn, J. W. Reiner, L. Mieville, T. H. Geballe, M. R. Beasley, and A. Kapitulnik, J. Phys.: Condens. Matter **8**, 10111 (1996).
[3] L. Klein, J. S. Dodge, C. H. Ahn, G. J. Snyder, T. H. Geballe, M. R. Beasley, and A. Kapitulnik, Phys. Rev. Lett. **77**, 2774 (1996).
[4] P. Kostic, Y. Okada, N. C. Collins, Z. Schlesinger, J. W. Reiner, L. Klein, A. Kapitulnik, T. H. Geballe, and M. R. Beasley, Phys. Rev. Lett. **81**, 2498 (1998).
[5] Y. Kats, I. Genish, L. Klein, J. W. Reiner, and M. R. Beasley, Phys. Rev. B **71**, 100403(R) (2005).
[6] Q. Gan, R. A. Rao, C. B. Eom, J. L. Garret, and M. Lee, Appl. Phys. Lett. **72**, 978 (1998).
[7] X. D. Wu, S. R. Foltyn, R. C. Dye, Y. Coulter, and R. E. Muenchausen, Appl. Phys. Lett. **62**, 2434 (1993).
[8] D. Toyota, I. Ohkubo, H. Kumigashira, M. Oshima, T. Ohnishi, M. Lippmaa, M. Kawasaki, and H. Koinuma, J. Appl. Phys. **99**, 08N505 (2006).
[9] D. Toyota, I. Ohkubo, H. Kumigashira, M. Oshima, T. Ohnishi, M. Lippmaa, M. Takizawa, and A. Fujimori, Appl. Phys. Lett. **87**, 162508 (2005).
[10] G. Herranz, F. Sánchez, M. V. Garcia-Cuenca, C. Ferrater, M. Varela, B. Martinez, and J. Fontcuberta, Mater. Res. Soc. Symp. Proc. **690**, F.3.5.1 (2002).
[11] M. Izumi, K. Nakazawa, and Y. Bando, J. Phys. Soc. Jpn. **67**, 651 (1998).
[12] J. W. Reiner, Ph.D. thesis, Stanford University, 2002.
[13] R. P. Borges, W. Guichard, J. G. Lunney, J. M. D. Coey, and F. Ott, J. Appl. Phys. **89**, 3868 (2001).
[14] J. Z. Sun, D. W. Abraham, R. A. Rao, and C. B. Eom, Appl. Phys. Lett. **74**, 3017 (1999).

[15] K. Fuchs, Proc. Cambridge Philos. Soc. **34**, 100 (1938).
[16] E. H. Sondheimer, Adv. Phys. **1**, 1 (1952).
[17] More generally: perpendicular to the projection of easy axis on the rotation plane.
[18] J. Thiele, C. Boeglin, K. Hricovini, and F. Chevrier, Phys. Rev. B **53**, R11934 (1996).
[19] U. Pustogowa, J. Zabloudil, C. Uiberacker, C. Blaas, P. Weinberger, L. Szunyogh, and C. Sommers, Phys. Rev. B **60**, 414 (1999).
[20] J.-W. Lee, J.-R. Jeong, S.-C. Shin, J. Kim, and S.-K. Kim, Phys. Rev. B **66**, 172409 (2002).
[21] J.-W. Lee, J. Kim, S.-K. Kim, J-.R. Jeong, and S.-C. Shin, Phys. Rev. B **65**, 144437 (2002).
[22] R. Allenspach, M. Stampanoni, and A. Bischof, Phys. Rev. Lett. **65**, 3344 (1990).
[23] A. Berger and H. Hopster, Phys. Rev. Lett. **76**, 519 (1996).
[24] D. P. Pappas, C. R. Brundle, and H. Hopster, Phys. Rev. B **45**, 8169 (1992).
[25] D. P. Pappas, K. P. Kämper, and H. Hopster, Phys. Rev. Lett. **64**, 3179 (1990).
[26] P. J. Jensen and K. H. Bennemann, Phys. Rev. B **42**, 849 (1990).
[27] D. Pescia and V. L. Pokrovsky, Phys. Rev. Lett. **65**, 2599 (1990).
[28] A. Moschel and K. D. Usadel, Phys. Rev. B **49**, 12868 (1994).
[29] Y. Kats, L. Klein, J. W. Reiner, T. H. Geballe, M. R. Beasley, and A. Kapitulnik, Phys. Rev. B **63**, 054435 (2001).
[30] F. Huang, G. J. Mankey, M. T. Kief, and R. F. Willis, J. Appl. Phys. **73**, 6760 (1993).
[31] D. Fuchs, T. Schwarz, O. Moran, P. Schweiss, and R. Schneider, Phys. Rev. B **71**, 092406 (2005).
[32] M. E. Fisher and A. E. Ferdinand, Phys. Rev. Lett. **19**, 169 (1967).
[33] G. A. T. Allan, Phys. Rev. B **1**, 352 (1970).
[34] M. E. Fisher and M. N. Barder, Phys. Rev. Lett. **28**, 1516 (1972).